ISBN: 978-3-95450-184-7 doi:10.18429/JACoW-IPAC2018-THPML136

STUDY OF SECONDARY ELECTRON GENERATION AND TRANSPORT IN DIAMOND

Tianlong He, Hongliang Xu*, Lin Wang, Zhiliang Ren, Derong Xu, Kaiting Huang
NSRL,USTC,Hefei,Anhui, China

Abstract

Energetic primary electrons (~ keV) impinging on the diamond film with its both surface under bias field in ~ MV/m, will excite secondary electron (SE) response including SE generation & transport. Although there have been 3D Monte Carlo (MC) simulation to study the two processes, this paper will introduce another method. Based on optical dielectric model, 3D MC simulation was implemented to study the generation process, and SE generation function was obtained by fitting the calculations. Using this function, the diffusion-drift equation of charge carriers (electron and hole) can be solved in 1D for the transport process, and the variation of SE depth distribution with time can be obtained.

INTRODUCTION

To satisfy the high requirements of Linac-based advanced light sources (X-FEL and ERL) for electron beam, like high average current and low transverse emittance, a diamond-amplifier photo-cathode injector scheme was proposed and under active development [1-3]. In this scheme, the initial electron beam produced by the conventional photo-cathode is firstly accelerated up to ~10 keV and then injected into the diamond film. Due to collision ionization, more than two orders of magnitude of SEs will be generated in diamond than the initial electrons, and the final amplified electron beam will be obtained by driving these SEs to emit into RF cavity. The process can be summarized as three stages: generation, transport and emission. This paper focused on the first two stages. For generation, we pay attention to the primary electron range and the depth distribution of SE, and get the generation function of SE by fitting this distribution. For transport, we solved the 1D diffusion-drift equation, and the variation of charge carrier distribution with time will be presented in detail.

METHODS

MC Simulation in 3D

MC method is extensively used to study particle transport in solids. The main processes involved are inelastic and elastic scattering. In our simulation, full Penn algorithm [4] (TPP model) was used to calculate the inelastic mean free path and the cumulative probability of energy loss of tracking electrons for inelastic scattering. Using these calculations, we can calculate the final energy of SE produced during inelastic. For elastic scattering, the NIST database [5] and Barbieri/Van Hove Phase Shift Package [6] were used to calculate the elastic mean free path and the scattering angle. The cut-off energy was set to 10 eV. The electron range, SE spatial distribution and SE generation function were mainly considered.

We have considered the following cases: 5 keV and 10 keV primary electron, no metal coating and coated metal of Pt in 30 nm.

Numerical Solution in 1D

The diffusion-drift equation can be described in a 1D form with the depth variable z taken as the coordinate normal to the diamond surface. Ignoring the carrier loss due to electron-hole recombination, the diffusion-drift equation can be drawn :

$$\frac{\partial n}{\partial t} = g \pm n\frac{\partial v}{\partial E}\nabla E + (\frac{\partial D}{\partial E}\nabla E \pm v)\nabla n + D\nabla^2 n \qquad (1)$$

where n(z, t) is the density distribution, g(z) is the generation function of charge carrier, v(E) is the drift velocity and D(E) is the diffusion coefficient. The plus and minus sign are used for electron and hole, respectively. Meanwhile the density of electron n_e and hole n_h should obey the Poisson equation:

$$\nabla^2\Phi = \frac{q(n_e - n_h)}{\varepsilon\varepsilon_0} \qquad (2)$$

Where Φ is the potential, ε=5.7 for diamond, and ε_0 is the vacuum permittivity, q is the elementary charge.

The diffusion-drift equation and Poisson equation can be solved by numerical algorithm with considering that the drift velocity and the diffusion coefficient are dependent on electric field E. v(E) can be expressed by an extensively used formula [7]:

$$v(E) = \frac{\mu_0 E}{1 + \mu_0 E / v_s} \qquad (3)$$

where μ_0 is the mobility under low field, and v_s is the saturation velocity. For diamond, $\mu_{e,0}$=250 nm^2/(V·fs), $\mu_{h,0}$=210 nm^2/(V·fs), $v_{s,e}$=0.15 nm/fs, and $v_{s,h}$=0.11 nm/fs [8,9] .

A fitted formula to describe the variation of electron longitudinal diffusion coefficient with field, derived from MC calculations by Osman [10], can be given by:

$$\ln(D_e) = \frac{p_1 \cdot \ln(E) + p_2}{\ln^2(E) + p_3 \cdot \ln(E) + p_4} \qquad (4)$$

where Eq. (4) was used when E>1500 V/cm, and D_e was considered as a constant 106 cm^2/s when E ≤ 1500V/cm. p_1=-7.628, p_2=155.6, p_3=-15.03,and p_4=77.85. For holes, D_h was assumed to be a constant 20 cm^2/s.

*hlxu@ustc.edu.cn

ISBN: 978-3-95450-184-7 doi:10.18429/JACoW-IPAC2018-THPML136

RESULTS

Maximum Electron Range

Figure 1 shows the electron ranges in diamond for 1~10 keV, which were obtained by MC calculation and an expression proposed by Kanaya and Okayama [11]. For 10 keV incident electron, the maximum electron range is <900 nm, which is far less than the spot diameter (~ 1 mm) of incident electron. Therefore, the diffusion-drift equation can be described in 1D form as Eq. (1).

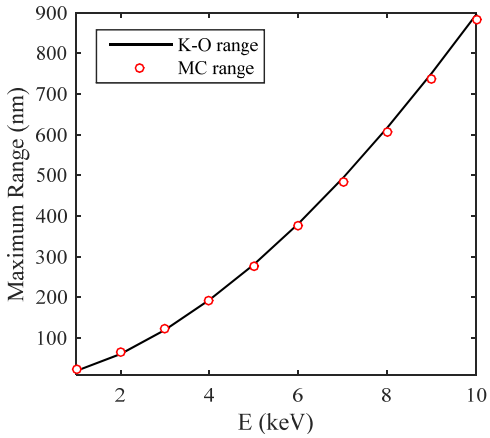

Figure 1: Electron range in diamond.

Spatial Distribution

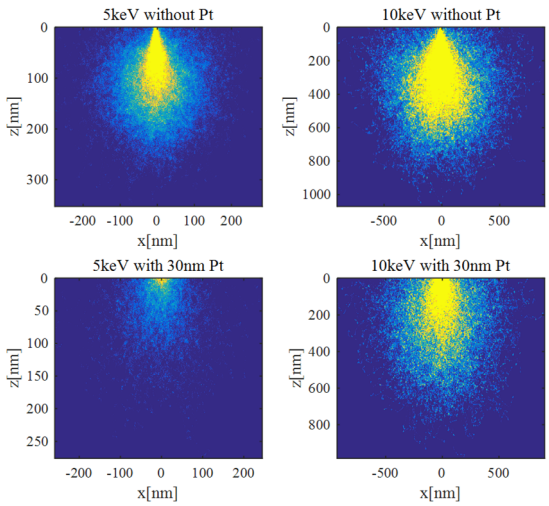

Figure 2: X-Z spatial distribution of SE generated in diamond by 5 keV and 10 keV incident electrons.

5000 initial electrons were tracked, and the final stop positions of all SEs were recorded. Their spatial distribution in X-Z plane and X-Y plane can be seen in Figs. 2 and 3, respectively. The title of every sub-figure gives the parameters for simulation: 5 keV and 10 keV denote the energy of primary electron, "without Pt" means the diamond film has no coated metal, and "with 30 nm Pt" means 30nm Pt is coated on the incident surface of the diamond.

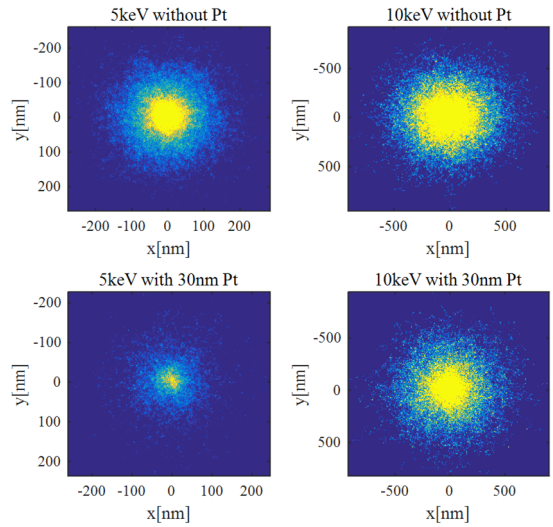

Figure 3: X-Y spatial distribution of SE generated in diamond by 5 keV and 10 keV incident electrons.

It can be seen that the coating of 30 nm Pt cause a significant energy loss especially for 5 keV incident electron. For 10 keV, no matter with or without Pt, the extension size is less than 900 nm and 1000 nm in longitudinal and transverse direction, respectively.

Generation Function

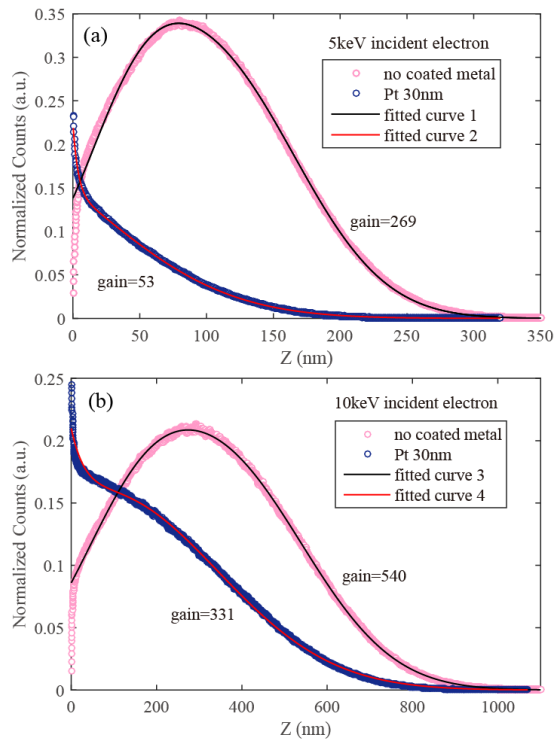

Figure 4: SE generation depth distribution for per incident electron with 5 keV (a), and 10 keV (b).

Figure 4 shows the MC results and the fitted curves. The integral of every curve is the SE yield. It can be seen that the coating of 30nm Pt significantly changed the distribution and reduced the gain more than 200 for 5keV and 10keV incident electron.

ISBN: 978-3-95450-184-7 doi:10.18429/JACoW-IPAC2018-THPML136

The curves in Fig. 4 are fitted by two terms of Gaussian function, can be expressed by:

$$g(z) = \sum_{i=1}^{2} a_i \cdot \exp(-(\frac{z-b_i}{c_i})^2) \quad (5)$$

where g(z) is the number of SE generated at the depth z as the same as that used in Eq. (1), the coefficients a, b, c are given in table 1, and Eq. (5) is the SE generation function, also can be taken as the hole generation function.

Table 1: Coefficients Fitted in Eq. (5)

Coe	Curve 1	Curve 2	Curve 3	Curve 4
a_1	0.0973	5.58E10	0.1814	1.08E10
b_1	44.07	-210.3	345.1	-1734
c_1	55.23	40.25	292.8	340.4
a_2	0.2925	0.1954	0.0643	0.1579
b_2	102.9	-74.24	131.5	72.84
c_2	93.21	136.1	194.5	381.2

Charge Carrier Transport

To study the variation of charge carrier distribution with time, the diamond film was set in thickness of 10 μm with a bias voltage of 40 V, and the time and space interval to 0.2 fs and 2 nm, respectively. Two kinds of initial beam were considered: one is pulsed with duration of 10 ps, interval ~ ns and charge 0.1 pC, and the other is continuous with current 10 μA.

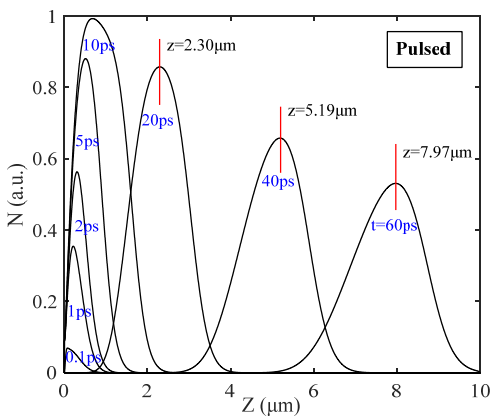

Figure 5: The depth distribution of electron varied with time.

For the pulsed, the variation was shown in Fig. 5. It is obvious that before 10ps the peak rose with time, meanwhile shifted rightward, after that time, it continued to decline and shifted rightward. The shifting velocity is about 0.142 μm/ps, which was calculated according to the Z positions of peak at 20 ps and 60 ps. The change of the peak was caused by the drift and diffusion effect of electron. The distribution was extended up to 5 μm at 60 ps due to the diffusion, however the initial distribution is less than 1 μm.

For the continuous beam, the results can be seen in Fig. 6. It is clear that the distribution of hole would get stable after 10 ps due to the combined effect of hole production and recombination. The holes drift towards the metal contact and are lost there under external field (~4 MV/m). However, a different variation was found for electron. The electron distribution continued to extend rightward and upward, after 10 ps, a flat-top shape appeared. The velocity of rightward extension can be evaluated according to the Z positions of half height at 20 ps and 60 ps, is 0.131 μm/ps.

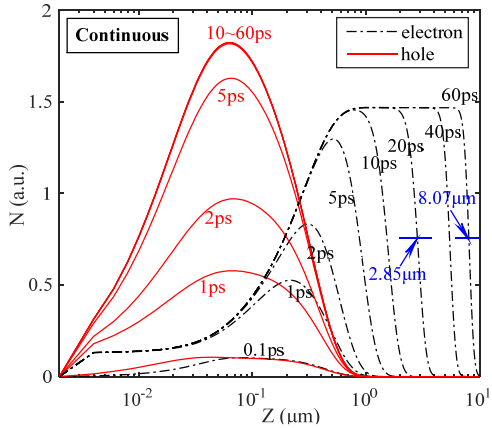

Figure 6: The depth distribution of electron and hole varied with time.

It is worth noting that the above results are dependent on the actual value of the saturated drift velocity and diffusion coefficient of electron.

CONCLUSION

Monte Carlo simulation for the SE generation process and numerical solution for the diffusion-drift equation of charge carrier have been conducted. The electron range of 10 keV is less than 900 nm, and its transverse extension size is less than 1000 nm, so the diffusion-drift equation can be described in 1D form. The depth distribution of SE was fitted well by two terms of Gaussian function, taken as the generation function of SEs as well as holes. The diffusion-drift equation of charge carrier had been solved using this generation function.

ACKNOWLEDGEMENT

This work is supported by the National Key Research and Development Program of China under Grant No.2016YFA0402001 and the National Nature Science Foundation of China under Grant Nos.11375176 and 10875118.

REFERENCES

[1] X. Chang. "Studies in Laser Photo-cathode RF Guns", Ph.D. thesis, Stoney Brook University, New York, USA, 2005.

[2] X. Chang *et al.*, "Electron beam emission from a diamond-amplifier cathode", Phys. Rev. Lett., vol. 105, p. 164801, 2010.

[3] D. A. Dimitrov *et al.*, "Multiscale three-dimensional simulations of charge gain and transport in diamond", J. Appl. Phys., vol. 108, 073712, 2010.

[4] S. Tanuma, C. J. Powell, and D. R. Penn, "Calculations of electron inelastic mean free paths. IX. Data for 41 elemental

ISBN: 978-3-95450-184-7 doi:10.18429/JACoW-IPAC2018-THPML136

solids over the 50 eV to 30 keV range ", Surf. Interface Anal. vol. 43, pp 689-713, 2011.

[5] NIST Electron Elastic Scattering Cross Section Database Version 4.0, https://srdata.nist.gov/SRD64/Elastic

[6] Barbieri A and Van Hove M, Phase Shift package, http://electron.lbl.gov/leedpack/

[7] J. Isberg, "Transport properties of electrons and holes in diamond", in CVD Diamond for Electronic Devices and Sensors, R.S. Sussmann, Ed. London, UK: Wiley, 1994, pp. 41

[8] F. Nava *et al.,* "Electron effective masses and lattice scattering in natural diamond", Solid State Commun., vol. 33, pp 475-477, 1980.

[9] L. Reggiani *et al.,* "Hole-drift velocity in natural diamond", Phys. Rev. B, vol. 23, pp 3050-3057, 1981.

[10] M. A. Osman et al., "Diffusion coefficient of electrons in diamond", Elsevier Science Publishers B.V., pp 611, 1991.

[11] J. I. Goldstein et al., "Scanning electron microscopy and X-Ray microanalysis", New York, NY, USA: Plenum Press, 1981, pp 72